

Hydration of POPC bilayers studied by ^1H -PFG-MAS-NOESY and neutron diffraction

Klaus Gawrisch · Holly C. Gaede ·
Mihaela Mihailescu · Stephen H. White

Received: 18 October 2006 / Revised: 1 February 2007 / Accepted: 8 February 2007 / Published online: 1 March 2007
© EBSA 2007

Abstract The stability of lipid bilayers is ultimately linked to the hydrophobic effect and the properties of water of hydration. Magic angle spinning (MAS) nuclear Overhauser enhancement spectroscopy (NOESY) with application of pulsed magnetic field gradients (PFG) was used to study the interaction of water with 1-palmitoyl-2-oleoyl-sn-glycero-3-phosphocholine bilayers in the fluid phase. NOESY cross-relaxation between water and polar groups of lipids, but also with methylene resonances of hydrophobic hydrocarbon chains, has been observed previously. This observation led to speculations that substantial amounts of water may reside in the hydrophobic core of bilayers. Here, the results of a quantitative analysis of cross-relaxation in a lipid 1-palmitoyl-2-oleoyl-sn-glycero-3 phosphocholine (POPC)/water mixture are reported. Coherences were selected via application of pulsed magnetic field gradients. This technique shortens acquisition times of NOESY spectra to 20 min and reduces t_1 -spectral noise, enabling detection of weak crosspeaks, like those between water and lipids, with higher precision than with non-gradient NOESY methods. The analysis showed that

water molecules interact almost exclusively with sites of the lipid–water interface, including choline, phosphate, glycerol, and carbonyl groups. The lifetime of lipid–water associations is rather short, on the order of 100 ps, at least one order of magnitude shorter than the lifetime of lipid–lipid associations. The distribution of water molecules over the lipid bilayer was measured at identical water content by neutron diffraction. Water molecules penetrate deep into the interfacial region of bilayers but water concentration in the hydrophobic core is below the detection limit of one water molecule per lipid, in excellent agreement with the cross-relaxation data.

Keywords POPC · Lipid · Membrane · Hydration · NMR · Neutron diffraction

Introduction

The interest in hydration of bilayers is driven by three observations: (i) the stability of bilayers results from the hydrophobic effect, an increase of the free energy of water upon contact with hydrophobic hydrocarbon chains (Tanford 1980). Therefore, understanding lipid–water interaction may shed light on the mechanisms responsible for assembly of lipids into bilayers. (ii) Fluid lipid bilayers have a surprisingly large permeability for water molecules, in particular bilayers of lipids with polyunsaturated hydrocarbon chains (Huster et al. 1997). On the order of one million water molecules per second pass through the lateral area of every phospholipid in a typical bilayer at physiological temperatures. Any movement of water through bilayers requires the presence of some water in the hydrophobic core. The mechanisms by which water molecules permeate bilayers are still debated (Disalvo et al. 1989). Therefore, understanding

Dedicated to Prof. K. Arnold on the occasion of his 65th birthday.

K. Gawrisch (✉)
Laboratory of Membrane Biochemistry and Biophysics,
NIAAA, NIH, Bethesda, MD 20892, USA
e-mail: gawrisch@helix.nih.gov

H. C. Gaede
Department of Chemistry, Texas A&M University,
College Station, TX, USA

M. Mihailescu · S. H. White
Department of Physiology and Biophysics,
University of California, Irvine, CA, USA

how water interacts with the lipid matrix may shed light on the mechanisms of water permeation. (iii) The chemical potential of water between two apposing bilayers at close approach is lower than that of bulk water. This potential translates into a substantial repulsive pressure between bilayers (LeNeveu et al. 1976). Several mechanisms may contribute to this repulsion. NMR investigations revealed that water molecules at the lipid water interface are partially oriented due to an interaction with the lipid water interface (Gawrisch et al. 1992) which could be the origin of a repulsive hydration force (Leikin and Kornyshev 1990). But the chemical potential of water may also be lowered by bilayer undulations (Helfrich 1978), by electrostatic repulsion between charged bilayers (Cowley et al. 1978) and by entropically driven movements of individual lipids or lipid segments along the bilayer normal (Israelachvili and Wennerström 1996). Repulsive forces between bilayers play a major role in cell fusion, one of the most fundamental biological processes (Arnold and Gawrisch 1993).

The systematic study of hydration of phosphatidylcholine (PC) bilayers began in the middle of the past century (Berendsen 1975). From early on, NMR played a major role in those investigations. Among the NMR studies, the work of Finer and Darke (Finer and Darke 1974), who investigated PC hydration by ^2H NMR as a function of water content, stands out. Their study revealed the existence of a pool of bulk water that is in slow exchange with water of hydration. The latter was divided into water trapped between bilayers, and up to three types of lipid-bound water. The dynamics of bound water are well fitted by a two-site exchange model with a primary hydration shell whose water molecules are influenced by interaction with lipid and a layer of free, unperturbed water in rapid exchange with the primary hydration shell (Borle and Seelig 1983; Volke et al. 1994).

The other pillar of hydration studies on bilayers are neutron and X-ray diffraction experiments. A clear advantage of diffraction methods is that they provide direct information on water density with resolution along the bilayer normal. The challenge has been to extract this information from bilayers in their biologically relevant liquid-crystalline state. Several laboratories have developed the experimental technology and reported data on water distribution (see, e.g., Franks and Lieb 1979; Simon et al. 1982; Wiener et al. 1991; Zaccai et al. 1979). Although, experiments were conducted on different lipids, with or without addition of cholesterol, and somewhat different levels of hydration, there is general agreement that water may penetrate into bilayers down to the level of hydrocarbon chain carbonyl groups, while water content in the hydrophobic bilayer center is below the detection limits.

Experiments conducted at the University of Leipzig under the leadership of Prof. Arnold linked the ^2H NMR

quadrupolar splitting of deuterated water to motions of water molecules in the membrane-bound state (Gawrisch et al. 1978). The model of water motions was derived from early molecular simulations of the lipid/water interface by the group of Frischleder (Frischleder and Peinel 1982). The ^2H NMR studies shed light on the mechanism of action of the water soluble polymer polyethylene glycol (PEG, MW = 8,000 or higher) that was widely used for induction of cell fusion at that time. Addition of PEG reduced the number of water molecules between bilayers (Arnold and Gawrisch 1993; Arnold et al. 1985), confirming earlier X-ray observations by Rand and Parsegian, that the PEG concentration near membrane surfaces is reduced, and PEG's addition to lipid/water dispersions reduces distances between bilayers via dehydration from osmotic stress (Parsegian et al. 1986).

The experiments also revealed that morphological changes in lipid water dispersions at water concentrations of fifteen water molecules per lipid and higher are the cause for a loss of resolution of $^2\text{H}_2\text{O}$ in the ^2H NMR spectra (Gawrisch et al. 1985). PCs at low water content typically form large, randomly oriented, flat arrays of bilayers. With increasing hydration, multilamellar liposomes of decreasing size are formed. With decreasing liposome size, lateral diffusion of water molecules over the curved surface of bilayers initially reduces resolution of ^2H NMR spectra and finally averages out quadrupolar splittings entirely. The effects are observable as soon as radii of curvature of lipid bilayers approach values on the order of 1 μm or less (Gawrisch et al. 1985).

Spherical liposomes cannot be packed without the formation of water-filled pockets between them. With increasing water concentration, both the thickness of water layers between lipid bilayers increases and the water-filled pockets enlarge. Eventually a balance between repulsive and attractive forces between bilayers is reached and any further addition of water increases the volume of water-filled pockets exclusively. The exact distribution of water between the interbilayer space and water-filled pockets depends somewhat on sample preparation methods, particularly at higher water content. This influence may explain conflicting reports about water uptake into the interbilayer space at water concentrations close to full hydration (Gawrisch et al. 1985; Klose et al. 1988).

More detail on sites of interaction with water as well as on water dynamics is accessible from ^1H NMR NOESY cross-relaxation measurements. Even the first NOESY experiments, conducted on small unilamellar liposomes produced by sonication, showed crosspeaks between water and lipid headgroup resonances (Xu and Cafiso 1986). Appearance of such crosspeaks requires a distance between water and lipid protons of 5 Å or less. After introduction of magic angle spinning (MAS) to NOESY experiments on

membranes, not only crosspeaks to headgroup resonances, but also to the methylene groups of lipid hydrocarbon chains were observed (Forbes et al. 1988). Volke and Pampel were the first to report that crosspeaks between the lipid 1-palmitoyl-2-oleoyl-sn-glycero-3-phosphocholine (POPC) and water at a concentration of nine water molecules per POPC have negative intensity, compared to positive intensity for all lipid–lipid crosspeaks (Volke and Pampel 1995). The laboratories of Stark and Epand confirmed that crosspeaks between water and lipid headgroups have negative intensity, but the crosspeak to the methylene resonance of hydrocarbon chains was weak and positive (Zhou et al. 1999). More recently we confirmed the latter observation in an experiment with coherence selection by pulsed magnetic field gradients (PFG) (Gaede and Gawrisch 2004).

Coherence selection by PFG reduces the acquisition time of 2D spectra up to a factor of eight. Furthermore, requirements for stability of MAS and spectrometer electronics are reduced, because coherence selection by PFG is complete within a fraction of a second, compared to ~30 s for coherence selection by phasing of rf-pulses. We recorded PFG-NOESY spectra at mixing times from 5 to 800 ms and performed a quantitative analysis of all water–lipid and lipid–lipid cross-relaxation rates by a matrix approach as described earlier (Huster et al. 1999). The quantitative analysis corrects for the wide intensity range of lipid and water resonances, as well as for the presence of relayed transfer of magnetization within the lipid matrix. The comparison of cross-relaxation rates on a per-proton basis yielded the sites and lifetimes of water–lipid association.

Finally, those NMR data were compared with the depth of water penetration into the POPC/water interface obtained by neutron diffraction on oriented POPC bilayers. Experiments were conducted as a function of humidity over the range from 66 to 93%. The water content of bilayers at 93% humidity is 9.4 ± 0.5 water molecules per lipid, within error limits identical to the water content of the NMR sample.

The experiments show that water associates for brief periods of time with polar groups of PC. The water content in the hydrophobic core of bilayers is less than one water molecule per lipid.

Materials and methods

NMR

The lipid 1-palmitoyl-2-oleoyl-sn-glycero-3 phosphocholine (POPC) (Avanti Polar Lipids, Alabaster, AL, USA)

was hydrated with deionized water, the lipid collected at the bottom of a sealed glass tube by centrifugation, and stored at ambient temperature for several hours to equilibrate water content. The pellet was transferred by centrifugation to a 4 mm MAS rotor that was fitted with inserts for liquid samples of a volume of 11 μ L (Bruker Biospin Corp., Billerica, MA, USA). NMR measurements were performed on a Bruker DMX500 widebore spectrometer at 500.17 MHz. The 4 mm PFG-MAS probe was operated at a MAS spinning frequency of 10 kHz. The gradients were supplied by a Bruker GREAT 3/10A amplifier. Sample temperature in the spinning rotor was calibrated by measuring the chemical shift difference between water and choline in a micellar sample of 1,2-dicaproyl-sn-glycero-3-phosphocholine (Avanti Polar Lipids; Alabaster, AL, USA) loaded into the 11 μ L spherical MAS rotor inserts that were used for experiments on model membranes. The chemical shift as a function of temperature was measured on the same sample in a 5 mm NMR tube using a high-resolution probe whose temperature had been calibrated precisely with a thermocouple.

Phase-sensitive NOESY experiments were acquired with two scans for each t_1 -increment. Experiments were conducted at mixing times from 5 to 800 ms at temperatures from 5 to 30°C. During the mixing time, a sine-shaped bipolar gradient pulse pair, separated by a 180°-proton pulse, was applied. Each gradient pulse had a length of 1 ms and a gradient strength of 0.23 T/m. The relaxation delay time d_1 was 4 s, with 128 t_1 -increments acquired at a spectral width of 10 ppm. The free induction decays were multiplied by a Gaussian window function in the f_2 domain and a shifted, squared sine-function in the f_1 domain. The base planes of Fourier transformed spectra were phase corrected by fitting the f_2 - and f_1 -domain data to polynomial functions of fifth order. No spectral symmetrization was applied.

For the quantitative determination of cross-relaxation rates, integral peak intensities were determined using routines in XWINNMR (Bruker Biospin, Billerica, MA, USA). Integral intensity of the weak crosspeaks between water and lipid resonances was determined by peak area analysis of the corresponding rows and columns in the 2D spectra. Spectra of rows and columns were baseplane corrected using the 1D baseplane correction routines of XWINNMR.

Cross-relaxation rates, normalized to the number of interacting protons per resonance, were calculated as reported previously (Huster et al. 1999). In brief, peak volume matrices $\mathbf{A}(t_m)$ and $\mathbf{A}(0)$ were assembled from the measured crosspeak intensities. The relaxation rate matrix \mathbf{R} was calculated from the normalized volume matrix $\mathbf{a}(t_m) = \mathbf{A}(t_m)(\mathbf{A}(0)^{-1})$ with the matrix of eigenvectors, \mathbf{X} , and the diagonal matrix of eigenvalues \mathbf{D} as

$$\mathbf{R} = -\frac{\mathbf{X}(\ln \mathbf{D})\mathbf{X}^{-1}}{t_m}, \quad (1)$$

where t_m is the mixing time.

Neutron diffraction

POPC multilayers were oriented on glass cover slips by evaporation of chloroform from a POPC/chloroform solution. Samples were dried in air and then in vacuum for 30 min to remove remaining traces of solvent. Before the experiments, samples were hydrated in the sealed spectrometer chamber for at least one hour, using saturated salt solutions. The samples were between 1,000 and 2,000 bilayers thick as calculated from the 1 to 2 mg of lipid deposited on an area of roughly 1 cm². This procedure yielded uniform, well oriented samples with a mosaic spread of less than 0.1°, as determined by rocking the sample in a neutron beam.

The neutron diffraction experiments were performed on the new Advanced Neutron Diffractometer/Reflectometer (AND/R) (Dura et al. 2006) located at the NIST Center for Neutron Research, Gaithersburg, MD (<http://www.ncnr.nist.gov/programs/reflect/ANDR>). The sample slides were mounted vertically in the neutron beam and kept under argon in a sealed enclosure throughout the experiments. The relative humidity was controlled by placing containers with saturated salt solutions into the sample chamber. Measurements were performed at four relative humidities: 66, 76, 86 and 93%, at room temperature. Under those conditions, the POPC is in a liquid-crystalline L_α phase. The deuterium content in the water of hydration was varied by exchanging H₂O for ²H₂O in the salt solutions. This method of water contrast variation enabled phasing of the bilayer structure factors, determination of the water distribution over the bilayer, scaling of the density profiles, and correction for extinction effects (Mihalescu and Gawrisch 2006). By performing θ - 2θ (specular) scans, the scattering-length density distribution in the direction normal to the bilayer plane was determined. Equilibration of the sample environment was established by following the time evolution of the peak positions and intensities in 1 h increments. Spectra, acquired after the equilibrium was reached, were summed up to improve signal-to-noise ratios for further analysis. The relative peak intensities bear the information on internal distribution of scattering length densities within a unit cell, i.e., a lipid bilayer. Fourier analysis of the Bragg diffraction intensities from the oriented POPC multilayers was employed (White et al. 1987; Worcester and Franks 1976) to determine bilayer structure. The water distribution was calculated by subtraction of scattering-length density profiles of samples with H₂O-²H₂O contrast variation.

Results

NOESY

The precise water content of the POPC/water sample was determined from a 1D ¹H MAS NMR spectrum. The integral intensity of the water resonance at 4.8 ppm was compared to integral intensity of the choline resonance at 3.3 ppm, which yielded a water content of 8.75 ± 0.25 water molecules per lipid. A 2D NOESY spectrum, acquired at a mixing time of 300 ms, is shown as contour plot in Fig. 1. Contours corresponding to positive intensities are shown in earthtone colors, and negative intensities in blue. While all lipid-lipid crosspeaks have positive intensity, the water crosspeaks to resonances of the lipid water interface are negative. Rows of the 2D-spectra showing crosspeaks between water and lipid resonances recorded as a function of mixing time are presented in Fig. 2. For comparison, the one-dimensional projection of a 2D NOESY spectrum, acquired at a mixing time of 5 ms and attenuated 256-fold, has been added at the top. The comparison of diagonal and crosspeak intensities shows that water-to-lipid crosspeaks have intensities in the range from 0.05 to 0.4% of the resonances on the spectral diagonal.

Intensity of crosspeaks between water and lipid resonances of the lipid/water interface, including choline α -, β -, and γ -resonance as well as glycerol g1, g2, and g3 are

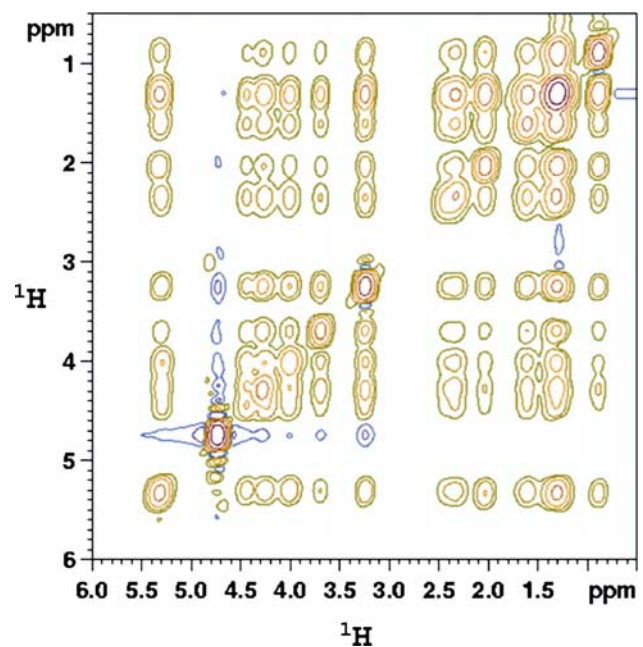


Fig. 1 Contour plot of a two-dimensional NOESY spectrum of the POPC/water dispersion, recorded at a mixing time of 300 ms and a temperature of 10°C. Contour levels with positive intensity are shown in earthtone colors and negative intensities in blue. Resonance assignments are provided in Fig. 2

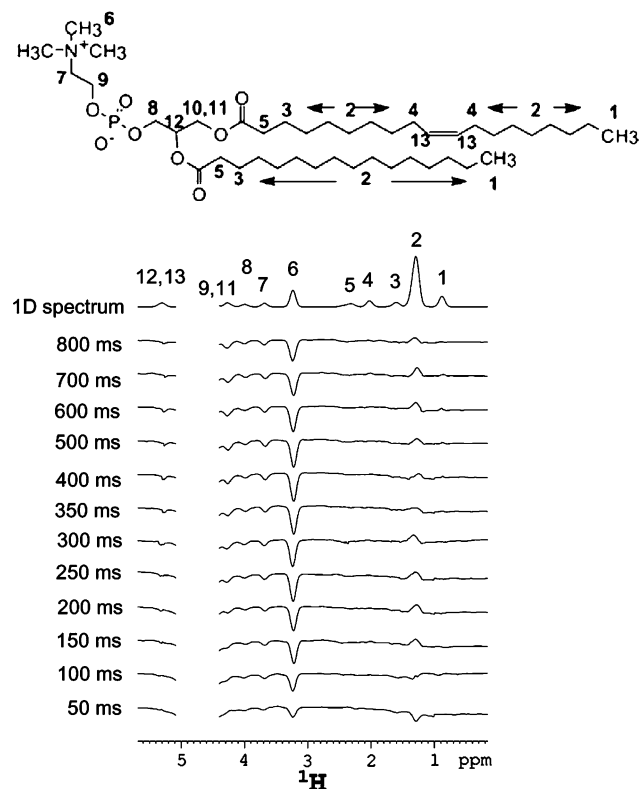


Fig. 2 Rows of two-dimensional NOESY spectra, recorded as a function of mixing time, showing water-to-lipid crosspeaks. The top spectrum is the 1D projection of a NOESY experiment, recorded at a mixing time of 5 ms. It shows the diagonal resonances, attenuated 256-fold. Resonance assignments are provided as numbers. The region of the intense water resonance was blended out for clarity

negative and increase in intensity up to mixing times of 400 ms. At longer mixing times intensity decreases again due to a loss of magnetization from spin-lattice relaxation. In contrast, the water crosspeak to the methylene resonances of hydrocarbon chains C_4 – C_{17} at 1.3 ppm is negative at the mixing time of 50 ms, has zero intensity at 100 ms, and becomes weakly positive at longer mixing times. Crosspeaks to hydrocarbon chain resonances C_2 and C_3 , to the resolved methylene resonance $-\text{CH}_2-\text{CH}=\text{CH}-\text{CH}_2-$ of the oleic acid chain, and to the terminal methyl groups of both chains were not detected. The change in sign of crosspeak intensity to the methylene resonance $-(\text{CH}_2)_n-$ as a function of mixing time is typical for contributions from relayed magnetization transfers that occur at longer mixing times.

The water resonance had minor wiggles near its base in the f_1 spectral domain, due to the small number of time increments that were acquired in the t_1 -domain. Therefore, crosspeaks in the rows of the 2D NOESY spectra tended to be less perturbed by minor spectral artifacts than crosspeaks in the columns. Their integral intensity was used for analysis of cross-relaxation rates

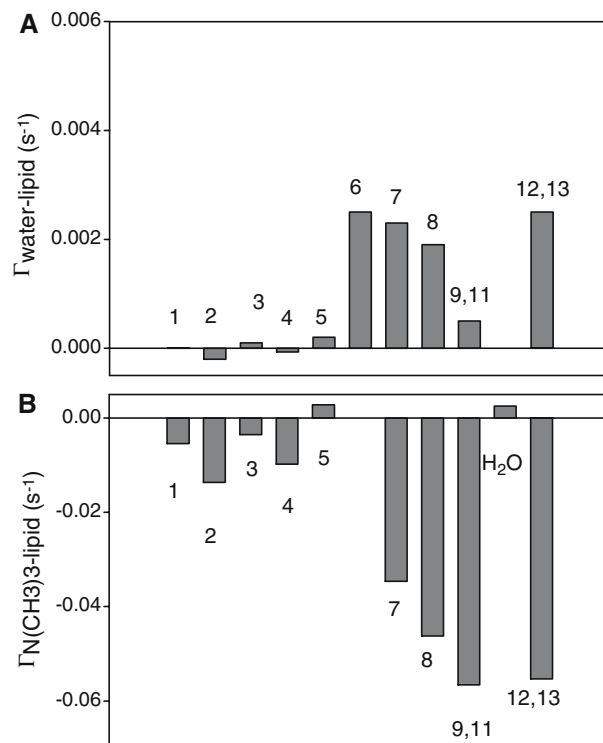


Fig. 3 **a** Normalized, per-proton cross-relaxation rates of magnetization transfer from water-to-lipid protons, $\Gamma_{\text{water-lipid}}$. Resonance assignments are provided as numbers (see Fig. 2). Cross-relaxation rates to protons of choline and glycerol groups are low and positive. All cross-relaxation rates to hydrocarbon chain resonances are very low. **b** Normalized, per-proton cross-relaxation rates of magnetization transfer from the choline methyl- to other lipid protons, $\Gamma_{\text{N(CH}_3)_3\text{-lipid}}$. Generally, those rates are negative. Please note that the y-scales of graphs **a** and **b** differ by one order of magnitude. Cross-relaxation rates from choline γ to resonances of the lipid-water interface are high. Weaker rates to lipid hydrocarbon chain resonances are observed as well. They reveal the tumultuous disorder in fluid lipid bilayers

as described in “Materials and methods”. The volume matrix $\mathbf{A}(0)$ was assembled from diagonal peak intensities acquired at the short mixing time of 5 ms to enable application of the pulsed field gradients during the mixing. Figure 3a shows all water-lipid cross-relaxation rates. For normalization of the cross-relaxation rate from water to the superimposed resonances of glycerol g2 and oleoyl chain double bond protons, it was assumed that only the glycerol resonance contributes to cross-relaxation. This assumption is supported by the slight off-center chemical shift of the crosspeak, in agreement with expectations for the chemical shift of glycerol g2. For comparison, choline γ -resonance cross-relaxation to all other lipid resonances is shown in Fig. 3b. While water-lipid cross-relaxation rates are very low and positive, all choline-lipid rates are negative and more than one order of magnitude larger. Please note that the y-scales of Fig. 3a, b differ by one order of magnitude.

Cross-relaxation was measured over the temperature range from 5 to 30°C in increments of 5°C. While lipid–lipid rates steadily increased in intensity with raising temperature as reported by us earlier (Yau and Gawrisch 2000), lipid–water cross-relaxation rates remained positive and displayed a small decrease of intensity (10–20%), barely outside experimental error limits.

Neutron diffraction

Diffraction from a stack of oriented lipid bilayers yields a coherently scattered neutron signal that was sampled as Bragg reflections at discrete angles θ . A Fourier analysis of the Bragg diffraction intensities bears the internal distribution of scattering length densities over the lipid bilayer and the adjacent water layers (Bacon 1975). For analysis, lipid multilayers are approximated as a collection of bilayer crystallites that are slightly misaligned with respect to an average plane (mosaic spread). In kinematical approximation, the coherently diffracted intensity, $I(n)$, at each diffraction order, n , is then related to the structure factor of a bilayer, $F(n)$, and the number of bilayers, N by the formula

$$I(n) \sim N^2 |F(n)|^2. \quad (2)$$

Since the natural diffraction peak width is broadened due to the instrumental resolution and the effective mosaic spread of the sample, the coherent reflected intensity at each Bragg order was determined by integrating the counts under the peak, $I(n)$, after background subtraction and absorption correction (Arndt and Willis 1966). The structure factors $F(n)$ are then determined as the square root of the peak integrals, corrected by the Lorentz factor, $\sin(2\theta_n)$, where θ_n represents the angle of incidence corresponding to the n th order of diffraction

$$|F(n)|^2 = (\sin(2\theta_n))I(n). \quad (3)$$

The approach is applicable to all diffraction orders if the diffraction power of the sample is modest (Bacon 1975; Bacon and Lowde 1948; Caspar and Philips). Those conditions are met when the sample thickness is below certain limits, or the isotopic contrast is appropriate. Dynamical diffraction effects (extinction) mostly influence the first diffraction order. Sample thickness was reduced and the proper corrections applied to eliminate an influence from extinction on data analysis (Bacon and Lowde 1948; Worcester D. L. et al., unpublished). The magnitude of structure factors decreases somewhat with increasing hydration due to increases in bilayer disorder (Hristova 1998; Wiener and White 1991a).

The scattering length density of the bilayer was determined from a Fourier sum of the bilayer structure factors, as

$$\rho(z) = \rho_0 + k \sum F(n) \cos(2\pi n z/d). \quad (4)$$

Because the bilayer constitutes a centro-symmetric crystal, there are only two possible phases corresponding to the sign, +1 or –1, of structure factors. Methods to determine those signs have been discussed in detail elsewhere (Blasie et al. 1975; Franks and Lieb 1979; Worcester and Franks 1976). We determined phases from measurements using H_2O – $^2\text{H}_2\text{O}$ contrast on samples containing at least three different mole fractions of $^2\text{H}_2\text{O}$. It was shown that the Fourier transform of the bilayer density is a linear function of the isotopic composition of water. Assuming a Gaussian distribution of water near the lipid headgroups, the difference structure factors corresponding to lipid hydrated with $^2\text{H}_2\text{O}$ or H_2O , respectively, are

$$\Delta F(n) = F_D - F_H \sim x_D \exp[-(\pi n A_1/d)^2] \cos\left(\frac{2\pi n Z_1}{d}\right), \quad (5)$$

where, A_1 and Z_1 denote the $1/e$ half-width and the mean position of the Gaussian distribution of the deuterated water, and x_D is the fraction of deuterium in the sample. Equation 5 was used to fit a single Gaussian line to the experimental difference structure factors, $\Delta F(n)$, corresponding to measurements in H_2O and $^2\text{H}_2\text{O}$, respectively. The position of the water layer was fixed to $d/2$, with the only fitted parameters being the $1/e$ half-width of the water distribution (A_w) and the scale factors, which are needed for placing the density profiles on an absolute, per-lipid scale, as described by Wiener and White (Wiener et al. 1991). The values of $\Delta F(n)$ obtained at 66, 76, 86, and 93% and their standard deviations are provided in Table 1. In Fig. 4 the scattering length density profile of the entire lipid bilayer and of water, acquired at a relative humidity of 93% are shown (Table 2).

Figure 5 reports the water distribution between two opposing POPC bilayers, corresponding to the four different levels of hydration. The dotted lines are the experimental profiles determined by direct subtraction of the scattering length density profiles determined for the spectrum acquired with $^2\text{H}_2\text{O}$ and H_2O , respectively. The solid black lines in Fig. 5 are the Gaussian profiles reconstructed with the parameters found from the fit. The number of waters per lipid corresponding to the four humidity conditions, as reported in Table 1, were determined previously (Hristova 1998; White et al. 1987). The uncertainty associated with water layer thickness was calculated based on the standard deviations of the experimental structure factors, using a Monte–Carlo sampling procedure as described by Wiener and White (Wiener and White 1992).

Table 1 Scaled difference structure factors, $\Delta F(n) = F(n; 20\% \text{ D}_2\text{O}) - F(n; \text{H}_2\text{O})$, and their standard deviations, SD, of POPC bilayers as a function of relative humidity (r.h.)

n	$\Delta F(n)$ (66% r.h.)	SD	$\Delta F(n)$ (76% r.h.)	SD	$\Delta F(n)$ (86% r.h.)	SD	$\Delta F(n)$ (93% r.h.)	SD
1	-3.63	0.05	-4.18	0.04	-4.9	0.03	-5.84	0.05
2	2.02	0.1	2.21	0.09	2.12	0.06	2.46	0.07
3	-0.71	0.11	-0.7	0.1	-0.61	0.07	-0.43	0.1
4	0.17	0.15	0.01	0.13	0.12	0.14	-0.03	0.28
5	-0.26	0.41	-0.03	0.26	-0.18	0.13	-0.04	0.33
6	0.02	0.27	0.02	0.35	0.02	0.32	0.01	0.67
7	0	0.5	0	0.46	0	0.54	0	0.69
8	0	0.46	0	0.43	0	0.41	0	0.79

n diffraction order, SD standard deviation

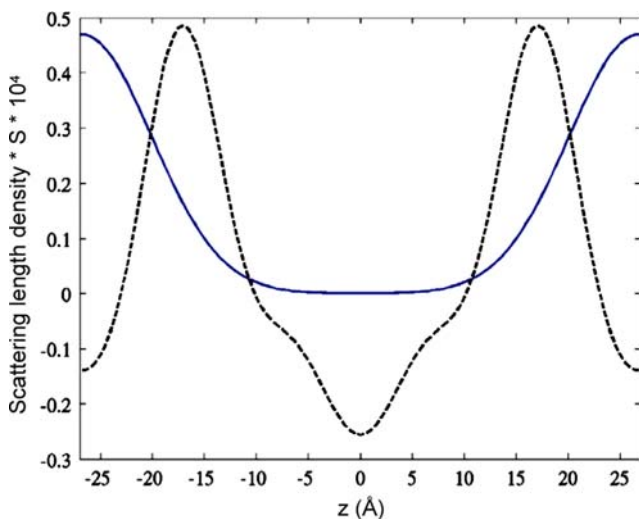


Fig. 4 Scattering length density (SLD) distributions of POPC and water along the bilayer normal, measured at a relative humidity of 93% and ambient temperature. The value $z = 0 \text{ \AA}$ corresponds to the bilayer center. The water density (blue) was calculated from the difference of density profiles recorded as a function of $^2\text{H}_2\text{O}$ content in the water of hydration (see “Results” for details)

Discussion

Water distribution from ^1H NOESY NMR

Water molecules have weak positive cross-relaxation rates with choline α -, β -, and γ -, as well as with glycerol g1-, g2-, and g3 resonances. Cross-relaxation rates to lipid hydrocarbon chain resonances are mostly below the detection limit. But a weak crosspeak to the very intense methylene resonance at 1.3 ppm was observed. Detection of this crosspeak is clearly favored by the large number of protons, 44, that contribute to this resonance. After normalization to the number of contributing protons, this rate is more than one order of magnitude lower than rates to

Table 2 Influence of relative humidity (r.h.) on the number of water molecules per POPC (n_w/lipid), bilayer repeat spacing (d), and the $1/e$ half-width of water layer thickness (A)

r.h. (%)	n_w/lipid	D (Å)	A (Å)
66	5.4	52.0 ± 0.1	7.48 ± 0.11
76	6.2	52.5 ± 0.1	7.81 ± 0.19
86	7.7	52.9 ± 0.1	8.80 ± 0.16
93	9.4	53.5 ± 0.1	9.22 ± 0.16

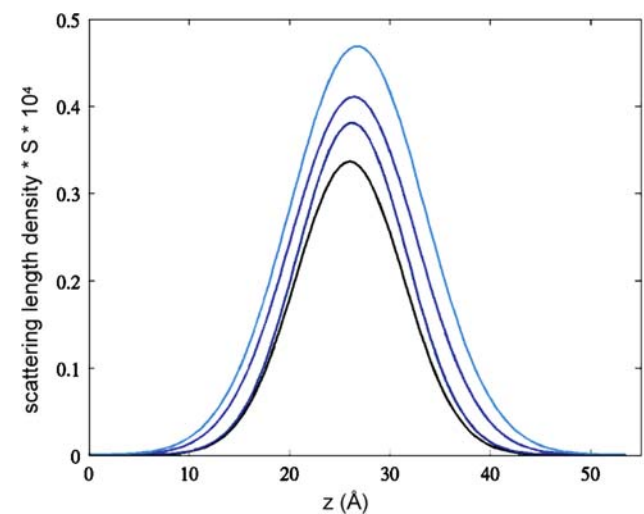


Fig. 5 Mean water distributions, determined as the difference scattering length densities of POPC measured in $^2\text{H}_2\text{O}$ and H_2O , respectively. The colors from dark to light blue correspond to hydration of POPC bilayers at relative the relative humidities 66, 76, 86, and 93%. With increasing water content, density of water and the thickness of the water layer increase. The center of the water layer moves somewhat closer to the bilayer center with increasing hydration. The latter is a reflection of a thinning of bilayers with increasing water content

hydrophilic protons of the lipid/water interface, strongly suggesting that water concentration in the hydrophobic core of bilayers is very low.

A deeper interpretation of cross-relaxation rates requires a discussion of their proton–proton distance dependence and their dependence on motional correlation times. NOESY cross-relaxation rates, Γ_{ij} , depend on the spectral density functions $J_{ij}(2\omega_0)$ and $J_{ij}(0)$ according to

$$\Gamma_{ij} = \zeta \left[3J_{ij}(2\omega_0) - \frac{1}{2}J_{ij}(0) \right], \quad (6)$$

where ω_0 is the proton Larmor frequency, and $\zeta = (2\pi 5) \gamma^4 \hbar^2 (\mu_0 4\pi)^2$, where γ is the gyromagnetic ratio of protons, and the other symbols have their usual meaning. Water–lipid and lipid–lipid cross-relaxation rates are determined both by the probability of close approach between protons and by changes in length and orientation of the vector connecting the interacting protons. The distance dependence stems from the amplitude factor $C_{ij}(0)$ that is proportional to $\left\langle \frac{1}{r_{ij}^6} \right\rangle$, where r_{ij} is the distance between interacting protons i and j . Because of the dependence on the sixth power of distance, the amplitude factor essentially counts events of very close approach between protons in the motionally disordered lipid matrix.

The functional dependence of Γ_{ij} on variation of proton–proton distances and orientation is comprehended most easily by assuming a single exponential decay of the correlation function, $C_{ij}(t)$, of proton–proton dipolar interaction:

$$\begin{aligned} C_{ij}(t) &= C_{ij}(0)e^{-t/\tau} \rightarrow J_{ij}(\omega) = \frac{2C_{ij}(0)\tau}{1 + \tau^2\omega^2} \rightarrow \Gamma_{ij} \\ &= C_{ij}(0)\zeta \left[\frac{6\tau}{1 + 4\tau^2\omega_0^2} - \tau \right] \end{aligned} \quad (7)$$

The first term in brackets of the equation for Γ_{ij} is from contributions with a spectral density $J_{ij}(2\omega_0)$ (see Eq. 6) These are motions with short correlation times in the range of picoseconds. They yield positive cross-relaxation rates. In contrast, the term, $-\tau$, is from slower motions related to the term $J_{ij}(0)$. At our proton Larmor frequency of 500 MHz, the positive and negative contributions to cross-relaxation cancel each other at a correlation time of ~ 400 ps. Shorter correlation times yield positive cross-relaxation rates and longer correlation times negative rates. Furthermore, the positive rates are low and reach a maximum at ~ 100 ps, while negative rates increase continuously with increasing length of the correlation time (Fig. 6).

Since water–lipid cross-relaxation rates are positive, they are dominated by water movements with correlation times on the order of 100 ps. Because the strength of dipolar interaction is significant only for distances between interacting protons of 5 Å or less, this time is essentially

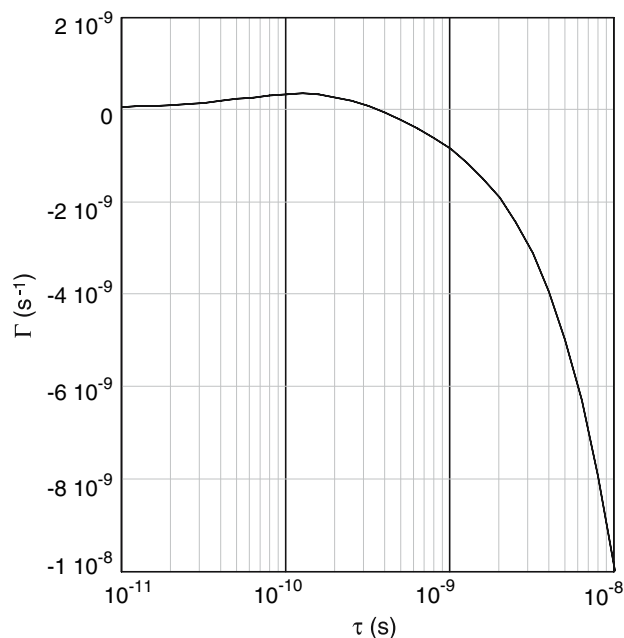


Fig. 6 Dependence of NOESY cross-relaxation rates on the correlation time, τ , of reorientation of the vector connecting the interacting protons. The dependence was calculated for a proton resonance frequency of 500 MHz. At correlation times $\tau < 400$ ps, cross-relaxation rates are positive. They reach a local maximum at $\tau \approx 100$ ps. At correlation times $\tau > 400$ ps, cross-relaxation rates are negative and increase steadily with increasing length of correlation times (see “Discussion” for details)

the lifetime of water association with a particular polar site in the lipid–water interface. With increasing temperature, those lifetimes get shorter, resulting in a small decline of cross-relaxation rates (Fig. 6), in excellent agreement with experimental observations.

Therefore, it is concluded that water molecules interact with sites in the polar lipid/water interface for brief periods of time, on the order of 100 ps, before moving on to the next site. The lifetime of ~ 100 ps agrees well with the correlation time of 110 ps for water molecules in the first hydration layer, obtained from spin–lattice relaxation time measurements on $^2\text{H}_2\text{O}$ in POPC (Volke et al. 1994).

If the lifetime of water–lipid associations would fall into a narrow range of correlation times near ~ 400 ps, the intensity of NOESY crosspeaks would vanish. But there are good reasons to believe that the lifetime of associations between water and hydrocarbon chains is shorter not longer than the 100 ps–lifetime of associations between water and polar headgroups. Typically, water immobilization at a particular site requires formation of at least one hydrogen bond. There are no sites for hydrogen bonding in the hydrophobic core. Furthermore, it can be expected that a change of temperature is sufficient to yield significant changes of crosspeak intensity or even a change of sign if correlation times are near 400 ps. However, changes of

crosspeak intensity over the temperature range of 5–30°C were barely measurable.

In contrast, the lipid–lipid cross-relaxation rates shown in Fig. 3b have a negative sign and are more than one order of magnitude larger. This indicates that correlation times of lipid proton–proton interactions are dominated by correlation times in the nanosecond range, more than one order of magnitude longer than correlation times of water–lipid interactions. Essentially, water molecules hop from site to site much faster than lipids change their conformation or separate from each other by lateral diffusion.

Water distribution from neutron diffraction

The scattering-length density profiles of Fig. 4 reveal directly that water penetration into the bilayer beyond the carbonyl groups is negligible. The dominant peaks in the hydrated POPC profile (dashed curve) are due almost exclusively to the carbonyl groups (Wiener and White 1991b, 1992), because they are the strongest neutron-scattering feature of the bilayer due to their lack of hydrogens with negative scattering lengths. In contrast, the equivalent dominant peaks in X-ray profiles are due to the electron-dense phosphate groups. The water profile in Fig. 4 (solid line) has decayed to almost 0 near the inner edges of the dominant carbonyl peaks.

The conclusion that water does not penetrate beyond the carbonyls to a significant extent is further supported by a simple calculation. The hydrophobic thickness of POPC bilayers, L , is conveniently estimated from average hydrocarbon chain order parameters of the saturated palmitic acid chain (Bloom and Mouritsen 1988; Nagle 1993) by the equation

$$L = 1.27 \times 2n(0.5 + S_{av}), \quad (8)$$

where n is the number of carbon atoms per palmitic acid chain, and S_{av} the average chain order parameter. We determined $S_{av} = 0.181$ by ^2H NMR on oriented POPC bilayers at conditions identical to those in the neutron diffraction experiments (Kimura and Gawrisch, unpublished). This calculation yields a hydrophobic bilayer thickness of 27.7 Å. Therefore, carbonyl groups of hydrocarbon chains are expected to be on average 13.8 Å away from the bilayer center. This is precisely the distance from the bilayer center at which water density begins to increase (Fig. 4). The lipid glycerol as well as choline protons are, on average, further away from the bilayer center and therefore well exposed to water.

The comparison with experiments on POPC bilayers at lower humidity shows that the location of the water layer as well as water layer thickness depend on relative humidity (see Table 1; Fig. 5). Those changes reflect not only an

increase of water layer thickness with increasing hydration, but also result from an increase of area per lipid molecule with increasing water content. It was shown earlier that low relative humidity is equivalent to compressing membranes laterally, which increases membrane hydrophobic thickness and reduces lateral area per molecule (Koenig et al. 1997). According to ^2H NMR measurements, the hydrophobic thickness of bilayers decreased to 27.1 Å at full hydration, compared to the 27.7 Å at 93% r.h. Although this change is significant, it does not alter principal conclusions regarding the penetration depth of water into POPC bilayers.

Summary

The average lifetime of water interactions with lipid carbonyl-, glycerol-, phosphate-, and choline groups in fluid lipid bilayers is on the order of 100 ps. The probability of deep water penetration into the hydrophobic core is rather low, as seen from the very low water–lipid cross-relaxation rates. Water–lipid cross-relaxation data are in excellent agreement with the more direct neutron diffraction data of water distribution over POPC bilayers that predict a water concentration in the hydrophobic core of less than one water molecule per lipid.

At first glance this observation is in disagreement with the high rates of water permeation through lipid bilayers. But high rates of transport do not necessarily translate into high water concentrations in the bilayer core. Let's assume that one million water molecules pass through the lateral area of one lipid per second. On average this corresponds to just one water molecule per lipid, per microsecond. If we consider that individual water molecules may pass through the bilayer in less than one microsecond, such relatively high permeation rates translate into very low water concentration in the hydrophobic core.

The time it takes a water molecule to pass through the core of a bilayer is related to water diffusion rates. For a hydrophobic core with a thickness of $x = 2.7$ nm and a time of permeation $t = 10^{-6}$ s, the diffusion rate is $D = x^2/2t = 3.6 \times 10^{-12} \text{ m}^2 \text{ s}^{-1}$. For comparison, the diffusion rate of water molecules in water at ambient temperature is about three orders of magnitude higher ($2.1 \times 10^{-9} \text{ m}^2 \text{ s}^{-1}$, Price et al. 1999). Even the lateral diffusion rate of POPC in bilayers [$8 \times 10^{-12} \text{ m}^2 \text{ s}^{-1}$, (Gaede and Gawrisch 2003)] is significantly higher. Therefore it is likely that water molecules pass through the hydrophobic core in a fraction of a microsecond and, consequently, the water concentration in the core of the bilayer is lower than one water molecule per lipid, in agreement with experimental observations.

When interpreting results of NMR and neutron scattering experiments it is important to remember that boundaries of

the hydrophobic core of fluid bilayers are not well defined. Lipid molecules are in tumultuous disorder (Wiener et al. 1991), up to the point that terminal methyl groups of hydrophobic hydrocarbon chains occasionally reach the lipid–water interface to exchange magnetization with the choline protons of neighboring lipid headgroups (Huster and Gawrisch 1999). Such choline-to-chain methyl crosspeaks were also observed for the POPC sample in this study (see Fig. 3). Therefore, the weak crosspeaks between water and hydrophobic methylene protons could be as much the result of infrequent chain upturns towards the lipid–water interface as the result of an occasional deep penetration of water molecules into the hydrophobic core. The low water content in the bilayer center suggests that water penetration through bilayers is very rapid. There is no evidence for a long-term association of water with any segment of lipids. The agreement between NOESY data and neutron diffraction results on water location is further proof that properly measured and normalized cross-relaxation rates are well suited for locating small molecules in bilayers.

Acknowledgments K.G. and H.G. were supported by the intramural program of NIAAA, NIH. The neutron diffraction studies were conducted on the AND/R instrument, constructed by the Cold Neutrons for Biology and Technology (CNBT) partnership, supported by the National Institute of Standards and Technology, the Regents of the University of California, and by a grant RR14812 from the National Institute for Research Resources awarded to the University of California at Irvine.

References

- Arndt UW, Willis BTM (1966) Single crystal diffraction. Cambridge University Press, Cambridge
- Arnold K, Gawrisch K (1993) Effects of fusogenic agents on membrane hydration: a deuterium nuclear magnetic resonance approach. *Methods Enzymol* 220:143–157
- Arnold K, Herrmann A, Pratsch L, Gawrisch K (1985) The dielectric properties of aqueous solutions of poly(ethylene glycol) and their influence on membrane structure. *Biochim Biophys Acta* 815:515–518
- Bacon GE (1975) Neutron diffraction, 3rd edn. Clarendon Press, Oxford
- Bacon GE, Lowde RD (1948) Secondary extinction and neutron crystallography. *Acta Cryst* 1:303–314
- Berendsen HJC (1975) In: Franks F (ed) *Water: a comprehensive treatise*, vol 5. Plenum Press, New York, London, pp 293
- Blasie JK, Schoenborn BP, Zaccai G (1975) Direct methods for the analysis of lamellar neutron diffraction from oriented multilayers: a difference Patterson deconvolution approach. *Brookhaven symposium in biology*, pp III–59
- Bloom M, Mouritsen OG (1988) The evolution of membranes. *Can J Chem* 66:706–712
- Borle F, Seelig J (1983) Hydration of *Escherichia coli* lipids. Deuterium T1 relaxation time studies of phosphatidylglycerol, phosphatidylethanolamine and phosphatidylcholine. *Biochim Biophys Acta* 735:131–136
- Caspar DL, Philips WC (1975) Dynamical effects in small angle neutron diffraction from membranes. *Brookhaven Symp Biol*, pp VII–107
- Cowley AC, Fuller NL, Rand RP, Parsegian VA (1978) Measurement of repulsive forces between charged phospholipid bilayers. *Biochemistry* 17:3163–3168
- Disalvo EA, Siddiqi FA, Tien HT, Benga G (1989) Membrane transport with emphasis on water and non-electrolytes in experimental lipid bilayers and biomembranes water transport in biological membranes, vol 1. CRC Press, Boca Raton
- Dura JA, Pierce DJ, Majkrzak CF, Maliszewskyj NC, McGillivray DJ, Losche M, O'Donovan KV, Mihailescu M, Perez-Salas U, Worcester DL, White SH (2006) AND/R: Advanced neutron diffractometer/reflectometer for investigation of thin films and multilayers for the life sciences. *Rev Sci Instrum* 77
- Finer EG, Darke A (1974) Phospholipid hydration studied by deuterium magnetic resonance spectroscopy. *Chem Phys Lipids* 12:1–16
- Forbes J, Husted C, Oldfield E (1988) High-field, high-resolution proton ‘magic-angle’ sample-spinning nuclear magnetic resonance spectroscopic studies of gel and liquid crystalline lipid bilayers and the effects of cholesterol. *J Am Chem Soc* 110:1059–1065
- Franks NP, Lieb WR (1979) Structure of lipid bilayers and the effects of general anesthetics—X-ray and neutron diffraction study. *J Mol Biol* 133:469–500
- Frischleder H, Peinel G (1982) Quantum-chemical and statistical calculations on phospholipids. *Chem Phys Lipids* 30:121–158
- Gaede HC, Gawrisch K (2003) Lateral diffusion rates of lipid, water, and a hydrophobic drug in a multilamellar liposome. *Biophys J* 85:1734–1740
- Gaede HC, Gawrisch K (2004) Multidimensional PFG-MAS-NMR experiments on membranes. *Magn Reson Chem* 42:115–122
- Gawrisch K, Arnold K, Gottwald T, Klose G, Volke F (1978) ²H NMR studies of the phosphate water interaction in dipalmitoylphosphatidylcholine/water systems. *Stud Biophys* 74:13–14
- Gawrisch K, Richter W, Möps A, Balgavy P, Arnold K, Klose G (1985) The influence of water concentration on the structure of egg yolk phospholipid/water dispersions. *Stud Biophys* 108:5–16
- Gawrisch K, Ruston D, Zimmerberg J, Parsegian VA, Rand RP, Fuller N (1992) Membrane dipole potentials, hydration forces, and the ordering of water at membrane surfaces. *Biophys J* 61:1213–1223
- Helfrich W (1978) Steric interaction of fluid membranes in multilayer systems. *Z Naturforsch* 33a:305–315
- Hristova K (1998) Determination of the hydrocarbon core structure of fluid dioleoylphosphocholine (DOPC) bilayers by X-ray diffraction using specific bromination of the double-bonds: Effect of hydration. *Biophys J* 74:2419–2433
- Huster D, Gawrisch K (1999) NOESY NMR crosspeaks between lipid headgroups and hydrocarbon chains: spin diffusion or molecular disorder? *J Am Chem Soc* 121:1992–1993
- Huster D, Jin AJ, Arnold K, Gawrisch K (1997) Water permeability of polyunsaturated lipid membranes measured by ¹⁷O NMR. *Biophys J* 73:855–864
- Huster D, Arnold K, Gawrisch K (1999) Investigation of lipid organization in biological membranes by two-dimensional nuclear Overhauser enhancement spectroscopy. *J Phys Chem B* 103:243–251
- Israelachvili J, Wennerström H (1996) Role of hydration and water structure in biological and colloidal interactions. *Nature* 379:219–225
- Klose G, Koenig BW, Meyer HW, Schulze G, Degovics G (1988) Small-angle X-ray scattering and electron microscopy of crude

- dispersions of swelling lipids and the influence of the morphology on the repeat distance. *Chem Phys Lipids* 47:225–234
- Koenig BW, Strey HH, Gawrisch K (1997) Membrane lateral compressibility determined by NMR and X-ray diffraction: effect of acyl chain polyunsaturation. *Biophys J* 73:1954–1966
- Leikin S, Kornyshev AA (1990) Theory of hydration forces—non-local electrostatic interaction of neutral surfaces. *J Chem Phys* 92:6890–6898
- LeNeveu DM, Rand RP, Parsegian VA (1976) Measurement of forces between lecithin bilayers. *Nature* 259:601–603
- Mihailescu M, Gawrisch K (2006) The structure of polyunsaturated lipid bilayers important for rhodopsin function—a neutron diffraction study. *Biophys J* 90:L4–L6
- Nagle JF (1993) Area/lipid of bilayers from NMR. *Biophys J* 64:1476–1481
- Parsegian VA, Rand RP, Fuller NL, Rau DC (1986) Osmotic stress for the direct measurement of intermolecular forces. *Methods Enzymol* 127:400–416
- Price WS, Ide H, Arata Y (1999) Self-diffusion of supercooled water to 238 K using PGSE NMR diffusion measurements. *J Phys Chem A* 103:448–450
- Simon SA, McIntosh TJ, Latorre R (1982) Influence of cholesterol on water penetration into bilayers. *Science* 216:65–67
- Tanford C (1980) *The hydrophobic effect: formation of micelles and biological membranes*. Wiley, New York
- Volke F, Pampel A (1995) Membrane hydration and structure on a subnanometer scale as seen by high-resolution solid-state nuclear magnetic resonance: POPC and POPC/C₁₂ EO₄ model membranes. *Biophys J* 68:1960–1965
- Volke F, Eisenblätter S, Galle J, Klose G (1994) Dynamic properties of water at phosphatidylcholine lipid-bilayer surfaces as seen by deuterium and pulsed-field gradient proton NMR. *Chem Phys Lipids* 70:121–131
- White S, Jacobs RE, King GI (1987) Partial specific volumes of lipid and water in mixtures of egg lecithin and water. *Biophys J* 52:663–665
- Wiener MC, White SH (1991a) Fluid bilayer structure determination by the combined use of X-ray and neutron diffraction. I. Fluid bilayer models and the limits of resolution. *Biophys J* 59:162–173
- Wiener MC, White SH (1991b) Fluid bilayer structure determination by the combined use of X-ray and neutron diffraction. II. Composition-space refinement method. *Biophys J* 59:174–185
- Wiener MC, White SH (1992) Structure of a fluid dioleoylphosphatidylcholine bilayer determined by joint refinement of X-ray and neutron diffraction data. III. Complete structure. *Biophys J* 61:434–447
- Wiener MC, King GI, White SH (1991) Structure of a fluid dioleoylphosphatidylcholine bilayer determined by joint refinement of X-ray and neutron diffraction data. I. Scaling of neutron data and the distributions of double bonds and water. *Biophys J* 60:568–576
- Worcester DL, Franks NP (1976) Structural analysis of hydrated egg lecithin and cholesterol bilayers. II. Neutron diffraction. *J Mol Biol* 100:359–378
- Xu ZC, Cafiso DS (1986) Phospholipid packing and conformation in small vesicles revealed by two-dimensional ¹H nuclear magnetic resonance cross-relaxation spectroscopy. *Biophys J* 49:779–783
- Yau WM, Gawrisch K (2000) Lateral lipid diffusion dominates NOESY cross-relaxation in membranes. *J Am Chem Soc* 122:3971–3972
- Zaccai G, Büldt G, Seelig A, Seelig J (1979) Neutron diffraction studies on phosphatidylcholine model membranes. II. Chain conformation and segmental disorder. *J Mol Biol* 134:693–706
- Zhou Z, Sayer BG, Hughes DW, Stark RE, Epand RM (1999) Studies of phospholipid hydration by high-resolution magic-angle spinning nuclear magnetic resonance. *Biophys J* 76:387–399